IJFAC

Indonesian Journal of Fundamental and Applied Chemistry

Article http://ijfac.unsri.ac.id

Synthesis and Characterization of Durian Peel Activated Carbon with Phosphoric Acid Activation for Direct Red 80 Adsorption

Gabri Ela Monica[1], Desnelli Desnelli[1,2,*], Ady Mara,[1,2]

[1] Master's Program in Chemistry, Faculty of Mathematics and Natural Sciences, Sriwijaya University, Jl. Raya Palembang Prabumulih KM 32 Inderalaya Ogan Ilir, Indonesia, 30662

[2] Departement of Chemistry, Faculty of Mathematics and Natural Sciences, Sriwijaya University, Jl. Raya Palembang Prabumulih KM 32 Inderalaya Ogan Ilir, Indonesia, 30662

Corresponding Author: nel_koto@yahoo.com

Abstract

This study aimed to synthesize, characterize, and evaluate the adsorption performance of H_3PO_4-activated carbon derived from durian peel for the removal of Direct Red 80. Durian peel was carbonized in a 750 W microwave oven for three heating cycles of 15 min each with 30 min cooling intervals and then activated using H_3PO_4 solutions at concentrations of 0.3, 0.4, and 0.5 M. Characterization was performed using Fourier Transform Infrared Spectroscopy (FTIR), X-Ray Diffraction (XRD), and analyses of moisture content, ash content, iodine adsorption capacity, methylene blue adsorption, and surface area determined based on the methylene blue adsorption method. FTIR analysis revealed the presence of O–H, aromatic C=C, and phosphate functional groups, while XRD indicated a predominantly amorphous carbon structure. Activation with 0.5 M H_3PO_4 produced activated carbon with the best characteristics, including a moisture content of 6.19%, ash content of 3.16%, iodine adsorption capacity of 1192.86 mg/g, exceeding the minimum requirement of SNI 06-3730-1995 (750 mg/g), and a surface area of 71.844 m^2/g determined by the methylene blue adsorption method. Adsorption was performed using 0.1 g adsorbent in 50 mL Direct Red 80 solution at 100 rpm. The optimum values obtained for the investigated parameters were pH 2, a contact time of 30 min, and an initial concentration of 30 ppm, with corresponding adsorption efficiencies of 66.72%, 66.72%, and 68.41%, respectively. The adsorption kinetics followed the pseudo-second-order model (R^2 = 0.9916), while the Langmuir model provided the best fit (R^2 = 0.9713). H_3PO_4-activated durian peel carbon shows potential as a biomass-based adsorbent for textile wastewater treatment.

Keywords: Activated carbon, Durian peel, Phosphoric acid, Direct Red 80, Adsorption

Article Info

Received 16 May 2026
Received in revised 2 June 2026
Accepted 5 June 2026
Available Online 30 June 2026

Abstrak (Indonesian)

Penelitian ini bertujuan untuk mensintesis, mengarakterisasi, dan mengevaluasi kemampuan adsorpsi karbon aktif kulit durian yang diaktivasi dengan asam fosfat (H_3PO_4) terhadap zat warna Direct Red 80. Kulit durian dikarbonisasi menggunakan oven microwave 750 W selama tiga siklus pemanasan masing-masing 15 menit dengan interval pendinginan 30 menit, kemudian diaktivasi menggunakan larutan H_3PO_4 dengan konsentrasi 0,3; 0,4; dan 0,5 M. Karakterisasi dilakukan menggunakan Fourier Transform Infrared Spectroscopy (FTIR), X-Ray Diffraction (XRD), serta analisis kadar air, kadar abu, daya serap iodin, adsorpsi metilen biru, dan luas permukaan yang ditentukan berdasarkan metode adsorpsi metilen biru. Hasil FTIR dan XRD menunjukkan keberadaan gugus fungsi O–H, C=C aromatik, dan fosfat serta struktur karbon yang didominasi fase amorf. Aktivasi menggunakan H_3PO_4 0,5 M menghasilkan karbon aktif dengan karakteristik terbaik, yaitu kadar air

6,19%, kadar abu 3,16%, daya serap iodin 1192,86 mg/g yang melampaui persyaratan minimum SNI 06-3730-1995 sebesar 750 mg/g, serta luas permukaan sebesar 71,844 m^2/g yang ditentukan berdasarkan metode adsorpsi metilen biru. Pengujian adsorpsi dilakukan menggunakan 0,1 g adsorben dalam 50 mL larutan Direct Red 80 pada kecepatan pengadukan 100 rpm. Nilai optimum yang diperoleh pada masing-masing variasi parameter adalah pH 2, waktu kontak 30 menit, dan konsentrasi awal 30 ppm dengan efisiensi adsorpsi berturut-turut sebesar 66,72%, 66,72%, dan 68,41%. Kinetika adsorpsi mengikuti model pseudo-orde dua (R^2 = 0,9916), sedangkan isoterm adsorpsi lebih sesuai dengan model Langmuir (R^2 = 0,9713). Karbon aktif kulit durian yang diaktivasi dengan H_3PO_4 berpotensi digunakan sebagai adsorben berbasis biomassa untuk pengolahan limbah cair tekstil.

Kata Kunci: Karbon aktif, Kulit durian, Asam fosfat, Direct Red 80, Adsorpsi

INTRODUCTION

Synthetic dyes are extensively used in the textile industry because of their bright colors, high stability, and ease of application. One of the commonly used dyes is Direct Red 80 (DR80), an anionic azo dye that is difficult to degrade naturally due to its complex molecular structure. The discharge of DR80-containing wastewater into aquatic environments can reduce water quality, disrupt aquatic ecosystems, and pose potential risks to human health because azo dyes may generate toxic and carcinogenic degradation products [1-3].

Among the various methods available for wastewater treatment, adsorption has attracted considerable attention because of its simplicity, relatively low operating cost, and high removal efficiency. Activated carbon is one of the most widely used adsorbents owing to its large surface area, well-developed pore structure, and abundant active sites that facilitate interactions with pollutant molecules [4]. However, commercial activated carbon is generally produced from non-renewable or relatively expensive raw materials, highlighting the need for alternative precursors derived from abundant and low-cost biomass resources.

Durian peel is a promising biomass waste to produce activated carbon. Indonesia produced approximately 1.71 million tons of durian in 2022, while durian peel accounts for about 60–75% of the total fruit weight, resulting in a substantial amount of underutilized biomass waste [5]. Durian peel contains cellulose, hemicellulose, and lignin, which are important components for carbon formation. The properties of activated carbon are strongly influenced by the activation process, particularly chemical activation. Among various chemical activating agents such as $ZnCl_2$, KOH, and H_3PO_4, phosphoric acid is widely used because it promotes pore development at relatively low activation temperatures while introducing oxygen-containing functional groups onto the carbon surface [6]. In addition, H_3PO_4 activation generally provides a higher carbon yield and minimizes excessive burn-off during activation [7,8]. These functional groups play an important role in enhancing the adsorption of dye molecules through electrostatic interactions, hydrogen bonding, and other adsorption mechanisms. Previous studies have reported that H_3PO_4-activated carbon exhibits high surface area and good adsorption performance toward various dye pollutants [8,9].

Previous studies have also demonstrated the potential of durian-derived materials for dye adsorption. Chandra *et al*. [10] reported that activated carbon prepared from durian shell exhibited good adsorption performance toward methylene blue and that the adsorption process could be adequately described using adsorption kinetic and isotherm models. In addition, durian peel has been investigated as a low-cost adsorbent for methylene blue removal from aqueous solutions, exhibiting favorable adsorption capacity and equilibrium characteristics. These findings indicate that durian-based adsorbents possess considerable potential for dye removal from wastewater. However, studies specifically investigating the adsorption of Direct Red 80 using H_3PO_4-activated durian peel carbon remain limited. Furthermore, information regarding the adsorption kinetics and isotherm behavior of Direct Red 80 on this adsorbent is still scarce. Therefore, further investigation is needed to evaluate its adsorption performance and adsorption behavior through kinetic and isotherm analyses. In addition, characterization techniques such as FTIR and XRD are important for identifying surface functional groups and structural properties of activated carbon, which may influence adsorption behavior and help explain the adsorption mechanism of Direct Red 80.

Based on these considerations, this study aimed to: (1) synthesize activated carbon derived from durian peel using different concentrations of H_3PO_4 as a chemical activating agent; (2) characterize the physicochemical properties of the prepared activated

carbon using FTIR and XRD analyses, as well as moisture content, ash content, iodine adsorption capacity, methylene blue adsorption, and surface area measurements; (3) evaluate the adsorption performance of Direct Red 80 under various adsorption conditions, including pH, contact time, and initial dye concentration; and (4) investigate the adsorption kinetics and adsorption isotherm behavior of Direct Red 80 on the prepared activated carbon.

MATERIALS AND METHODS

Materials

The materials used in this study included durian peel (*Durio zibethinus* Murr.) obtained from local durian vendors in Palembang, South Sumatra; 85% phosphoric acid (H_3PO_4) p.a. (Merck), distilled water as a solvent, solid iodine (I_2), potassium iodide (KI) p.a., 0.1 N sodium thiosulfate ($Na_2S_2O_3$), potassium iodate (KIO_3) p.a. for standardization, and 1% starch indicator.

Methods

Preparation of durian peel

The durian peel was washed with clean water to remove dirt and residual fruit pulp, then cut into pieces of approximately 1–2 cm. The samples were subsequently dried in an oven at 105 °C for 3 hours to reduce the moisture content before further processing.

Preparation of activated carbon

The dried durian peel was placed in a domestic microwave oven (Sharp R-2100M, 750 W, 2450 MHz) and carbonized under ambient atmospheric conditions. The carbonization process was carried out in three heating cycles, each consisting of 15 min of heating followed by a 30 min cooling interval. After completion of the carbonization process, the resulting charcoal was cooled to room temperature, ground, and sieved using an 80-mesh sieve to obtain a uniform particle size. The sieved charcoal was subsequently stored in a sealed container prior to the activation process.

Activation of activated carbon

The carbonized material was treated with phosphoric acid (H_3PO_4) solutions at concentrations of 0.3, 0.4, and 0.5 M. Ten grams of durian peel charcoal were soaked in the activating solution using a charcoal-to-solution ratio of 1:10 (g/mL). The soaking process was carried out for 24 h at room temperature to facilitate the penetration and distribution of the activating agent within the carbon structure

After the treatment process was completed, the samples were filtered and washed with distilled water until a neutral pH (± 7) as determined using universal pH indicator paper, to ensure the removal of residual phosphoric acid. The samples were then dried in an oven at 115 °C for 12 h. The dried activated carbon was subsequently ground and sieved through an 80-mesh sieve to obtain a uniform particle size. The sieved activated carbon was stored in a sealed container prior to further characterization and adsorption experiments

Moisture content determination

A 1 g sample of activated carbon was dried in an oven at 115 °C for 3 hours. The sample was then cooled in a desiccator until a constant weight was reached and subsequently weighed. Moisture content analysis was carried out according to SNI 06-3730-1995, and the moisture content was determined based on the difference in mass before and after drying.

Ash content determination

A 1 g sample of activated carbon was heated in a furnace at 800 °C for 2 hours until complete ash formation occurred. The sample was then cooled in a desiccator until a constant weight was reached and subsequently weighed. Ash content analysis was carried out according to SNI 06-3730-1995, and the ash content was determined based on the ratio of ash mass to the initial sample mass.

Iodine adsorption capacity determination

A total of 0.5 g of activated carbon was dried in an oven at 115 °C for 1 h and then cooled in a desiccator for 15 min. The sample was transferred into an Erlenmeyer flask, followed by the addition of 25 mL of 0.1 N iodine solution. The mixture was shaken at 200 rpm for 15 min at room temperature, then centrifuged and filtered to obtain a clear filtrate. Subsequently, a 10 mL aliquot of the filtrate was titrated with 0.1 N sodium thiosulfate ($Na_2S_2O_3$) solution until the solution became pale yellow. A few drops of 1% starch indicator were then added, and the titration continued until the blue color disappeared. A blank solution was prepared using the same procedure. All measurements were performed in duplicate [11] :

$$\text{Iodine adsorption capacity} = \frac{(V1\text{-}V2)\text{x N x Ar x fp}}{W} \quad \ldots\ldots(1)$$

where:

(V1) : volume of sodium thiosulfate used for blank titration (mL)
(V2) : volume of sodium thiosulfate used for sample titration (mL)
(N) : normality of sodium thiosulfate solution
(126.93) : atomic weight of iodine(g/mol)
(fp) : dilution factor (5)
(W) : mass of activated carbon used (g)

Methylene Blue surface area determination

A total of 0.1 g of activated carbon was mixed with 25 mL of 100 ppm methylene blue solution in a 250 mL Erlenmeyer flask covered with aluminum foil. The mixture was stirred using a magnetic stirrer at 100 rpm for 30 minutes at room temperature. Subsequently, the mixture was filtered, and the remaining methylene blue concentration in the filtrate was measured using a UV-Vis spectrophotometer at the maximum wavelength. The adsorption of methylene blue was used to estimate the surface area of activated carbon. The amount of adsorbed methylene blue was calculated using the following equation [12]:

$$Xm = \frac{(Co\text{-}Ce) \times Vsolution}{\text{mass of activated carbon}} \quad \text{.....(2)}$$

Where:

Xm : amount of adsorbed methylene blue (mg/g)
Co : initial concentration of methylene blue solution (mg/L)
Ce : final concentration of methylene blue solution (mg/L)
V : volume of methylene blue solution (L)
m : mass of activated carbon (g)

$$S = \frac{(Xm.\ N.\ A)}{Mr} \quad \text{.....(3)}$$

Where:

S : surface area of activated carbon (m^2/g)
Xm : amount of adsorbed methylene blue (mg/g)
N : Avogadro's number ((6.02×10^{23} molecules/mol)
A : cross-sectional area of methylene blue molecule ((197×10^{-20} m^2/molecule)
Mr : molecular weight of methylene blue (319.85 g/mol).

Activated carbon characterization

Activated carbon was characterized using Fourier Transform Infrared Spectroscopy (FTIR) with a Shimadzu IRTracer-100 instrument. The crystal structure of the activated carbon was analyzed using X-ray Diffraction (XRD) with a SmartLab Rigaku instrument.

Determination of the point of zero charge (pHpzc)

Determination of pHpzc was carried out by adding 50 mL of 0.01 M NaCl solution into a 100 mL beaker. The initial pH of the solution was adjusted to a range of 2–12 using 0.1 M HCl and 0.1 M NaOH. Subsequently, 0.1 g of activated carbon was added to the solution, and the mixture was shaken in a shaker bath for 2 hours and allowed to stand for 24 hours at room temperature. Afterward, the solution was filtered, and the final pH was measured using a pH meter to determine the pHpzc value of the activated carbon.

Adsorption test

The adsorption performance of activated carbon toward Direct Red 80 was evaluated by varying the solution pH (2–6), contact time (20–60 min), and initial dye concentration (20–60 mg/L). The optimization experiments were conducted using a one-factor-at-a-time (OFAT) approach, in which one parameter was varied while the remaining experimental conditions were kept constant. During pH and contact time optimization, the initial dye concentration was maintained at 20 mg/L. During concentration optimization, the solution pH and contact time were fixed at the optimum values obtained from the previous experiments. The adsorbent mass (0.1 g) and solution volume (50 mL) were kept constant throughout all adsorption experiments.

Adsorption experiments were carried out by mixing 0.1 g of activated carbon with 50 mL of Direct Red 80 solution in a 100 mL Erlenmeyer flask. The solution pH was adjusted to the desired value using dilute HCl and NaOH solutions prior to the adsorption experiments. The mixture was agitated using a shaker at 100 rpm at room temperature for a predetermined contact time. After adsorption, the mixture was filtered using filter paper, and the residual dye concentration in the filtrate was determined using a UV–Vis spectrophotometer at the maximum wavelength (λmax) of 528 nm. All adsorption experiments were performed in duplicate, and the reported values represent the average of the obtained results. The adsorption capacity (Qe) and removal efficiency (R%) were calculated using the following equations [13]:

$$Qe = \frac{(Co\text{-}Ce) \times V}{m} \quad \text{.....(4)}$$

$$R\,(\%) = \frac{Co\text{-}Ce}{Co} \times 100\% \quad \text{.....(5)}$$

Where:

Co : the initial concentrations of Direct Red 80 (mg/L)
Ce : equilibrium concentrations of Direct Red 80 (mg/L)
V : volume of solution (L)
m : mass of adsorbent (g).

Adsorption kinetics

Adsorption kinetics were studied to evaluate the adsorption rate of Direct Red 80 by durian peel activated carbon based on the relationship between contact time and adsorption capacity (qt). The kinetic study was conducted under optimum adsorption conditions at pH 2 using 0.1 g of adsorbent and 50 mL of 30 ppm Direct Red 80 solution at room temperature with agitation at 100 rpm using a shaker. The adsorption data were analyzed using pseudo-first-order and pseudo-second-order kinetic models. The linear

form of the pseudo-first-order model is expressed as follows [14]:

$$\log(q_e - q_t) = \log q_e - \frac{k_1}{2.303} t \quad \text{.....(6)}$$

Where:
qe and qt represent the adsorption capacities at equilibrium and at time (t) (mg/g), respectively, while (k_1) is the pseudo-first-order rate constant (min^{-1}). The linear form of the pseudo-second-order model is expressed as follows:

$$\frac{t}{q_t} = \frac{1}{k_2 q_e^2} + \frac{t}{q_e} \quad \text{.....(7)}$$

Where:
K_2 is the pseudo-second-order rate constant (g/mg·min). The suitability of each kinetic model was evaluated based on the coefficient of determination R^2 and the consistency of the obtained parameters.

Adsorption isotherm models

The adsorption isotherm was determined based on the relationship between the equilibrium concentration (C_e) and the adsorption capacity (Q_e) at various concentrations of Direct Red 80 solution. The data obtained were used to evaluate the suitability of the Langmuir and Freundlich isotherm models. In the Langmuir model, C_e/Q_e was plotted against C_e to determine the parameters Q_m and K_l from the linear equation. Meanwhile, in the Freundlich model, log Q_e was plotted against log C_e to determine the values of K^f and 1/n. The suitability of both models was evaluated based on the coefficient of determination (R^2). The most appropriate model was identified from the highest R^2 value

RESULTS AND DISCUSSION

Synthesis of durian peel activated carbon

In this study, activated carbon was prepared from durian peel waste through a microwave-assisted carbonization process. During carbonization, lignocellulosic components such as cellulose, hemicellulose, and lignin were decomposed into carbon-rich material. The carbonization process produced a dark black char with a more brittle texture compared to the raw durian peel. These changes indicate the formation of carbonaceous material due to the release of volatile compounds during the heating process [15,16].

Figure 1 shows the color change of durian peel from yellowish-brown to black after the carbonization process. The darker color indicates the transformation of biomass into carbon-rich material as a result of thermal decomposition during heating. In addition, the more brittle texture of the material suggests that the original biomass structure had undergone substantial degradation, leading to the formation of char [16].

Figure 1. Activated carbon derived from durian peel waste

Microwave-assisted carbonization reduced the mass of dried durian peel from 5.0019 g to 2.4887 g, corresponding to a carbonization yield of 49.75%. The reduction in mass reflects the thermal degradation of lignocellulosic components and the release of volatile compounds during carbonization, resulting in the formation of carbon-rich material. Similar reductions in biomass mass during carbonization have been reported and are associated with the decomposition of cellulose, hemicellulose, and lignin fractions [17,18]. Carbonization was carried out using a microwave oven (Sharp, 750 W). Microwave-assisted carbonization enables rapid heating of biomass, facilitating the conversion of lignocellulosic materials into carbonaceous products within a relatively short processing time compared with conventional heating methods [1, 19].

Activation of activated carbon using phosphoric acid (H_3PO_4)

The carbonized material was subsequently treated with phosphoric acid (H_3PO_4) at concentrations of 0.3, 0.4, and 0.5 M. The treatment was carried out by immersing the carbonized material in the acid solution for 24 h at room temperature, followed by washing with distilled water until neutral pH and drying at 115 °C.

After the treatment process, a decrease in carbon mass was observed at each concentration variation. At a concentration of 0.3 M, the carbon mass decreased from 10.001 g to 8.7581 g, corresponding to a yield of 87.57%. At 0.4 M, the mass decreased from 10.003 g to 8.7693 g, resulting in a yield of 87.67%, while at 0.5 M, the mass decreased from 10.0005 g to 8.4052 g, corresponding to a yield of 84.05%.

The reduction in carbon mass indicates that some components of the carbonized material were removed during the treatment and washing processes. Acid

treatment has been reported to alter the composition of carbon materials through interactions between the acid and the carbon matrix, resulting in the removal of certain inorganic constituents and other acid-soluble components [20, 21]. The carbon yield obtained in this study remained relatively high, ranging from 84.05% to 87.67%, indicating that most of the carbonized material was retained after treatment. The yields at 0.3 and 0.4 M were relatively similar, whereas the lowest yield was obtained at 0.5 M. This result suggests that treatment with 0.5 M H_3PO_4 had a greater effect on the carbonized material than the lower concentrations, resulting in a higher mass loss after the treatment and washing processes.

Moisture content of activated carbon

The moisture content test results of activated carbon activated using phosphoric acid (H_3PO_4) after drying at 115 °C for 3 h were 6.82283%, 5.84754%, and 6.1928% at H_3PO_4 concentrations of 0.3, 0.4, and 0.5 M, respectively. All obtained moisture content values were below the maximum limit specified by SNI 06-3730-1995 (15%), indicating that the produced activated carbon met the required quality standard.

As shown in **Figure 2**, the moisture content varied among the samples. The lowest value was obtained at an H_3PO_4 concentration of 0.4 M, whereas slightly higher values were observed at 0.3 and 0.5 M. No regular trend in moisture content was observed with increasing H_3PO_4 concentration.

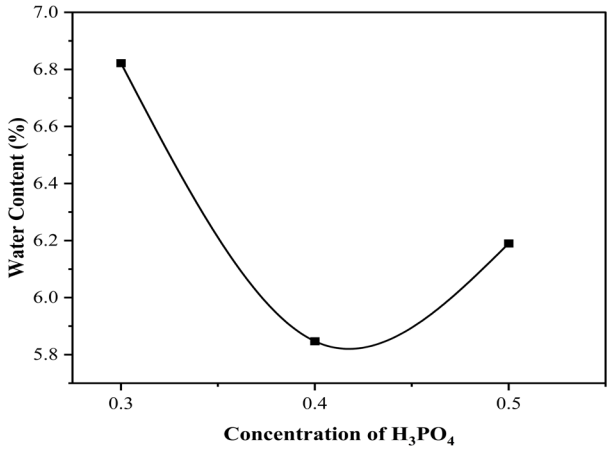

Figure 2. Moisture content of durian peel activated

Ash content of activated carbon

The ash content test results of activated carbon treated with phosphoric acid (H_3PO_4) were 1.252601%, 1.26377%, and 3.160559% at H_3PO_4 concentrations of 0.3, 0.4, and 0.5 M, respectively. All obtained ash content values were below the maximum limit specified by SNI 06-3730-1995 (10%), indicating that the produced activated carbon met the required quality standard.

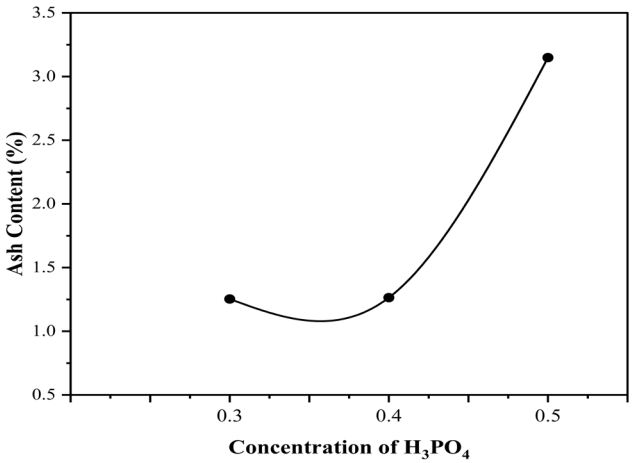

Figure 3. Ash content test results of durian peel activated carbon activated with phosphoric acid

Based on **Figure 3**, the ash content values at H_3PO_4 concentrations of 0.3 and 0.4 M were relatively similar, whereas a higher ash content was observed at 0.5 M. These results indicate that increasing H_3PO_4 concentration was not accompanied by a regular increase in ash content. Ash content is commonly used as an indicator of the inorganic residue remaining in activated carbon, and low ash content is generally preferred because it reflects the quality of the adsorbent [22].

Determination of iodine adsorption capacity of durian peel activated carbon

The iodine adsorption test results of durian peel activated carbon treated with phosphoric acid (H_3PO_4), as shown in **Figure 4**, were 1173.83 mg/g at H_3PO_4 concentrations of 0.3 and 0.4 M and 1192.86 mg/g at 0.5 M. All obtained iodine adsorption values exceeded the minimum requirement specified by SNI 06-3730-1995 (750 mg/g), indicating that the produced activated carbon met the quality standard for iodine adsorption capacity.

As shown in **Figure 4**, the iodine adsorption values obtained at different H_3PO_4 concentrations were relatively similar, ranging from 1173.83 to 1192.86 mg/g. The highest value was obtained at an H_3PO_4 concentration of 0.5 M. Previous studies have reported iodine adsorption capacities of 698.12 mg/g for bamboo-based activated carbon [11] and 666.73 mg/g for durian peel activated carbon [23]. Differences in iodine adsorption capacity among studies may be related to variations in raw materials and experimental conditions used during activated carbon preparation [24].

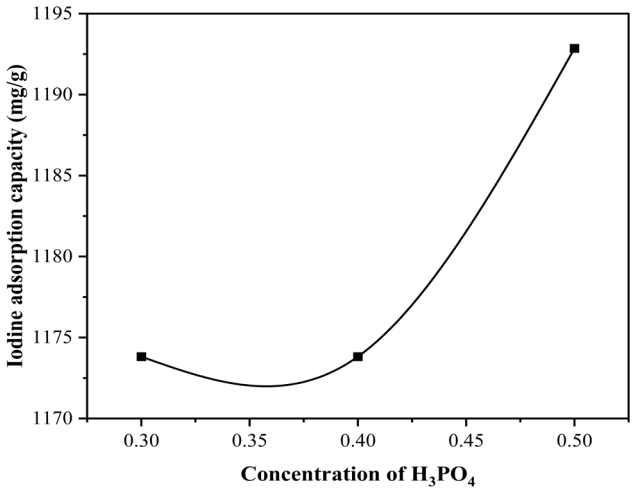

Figure 4. Iodine adsorption test results of durian peel activated carbon activated with phosphoric acid

Determination of surface area of durian peel activated carbon

The surface area of activated carbon was determined using the methylene blue adsorption method based on the relationship between the concentration and absorbance of the standard solution. As shown in **Figure 5**, an increase in methylene blue concentration was accompanied by an increase in absorbance. The calibration curve produced a linear regression equation with a coefficient of determination (R^2) of 0.9884. An R^2 value close to 1 indicates a strong linear relationship between concentration and absorbance, allowing the regression equation to be used for calculating the surface area of the activated carbon.

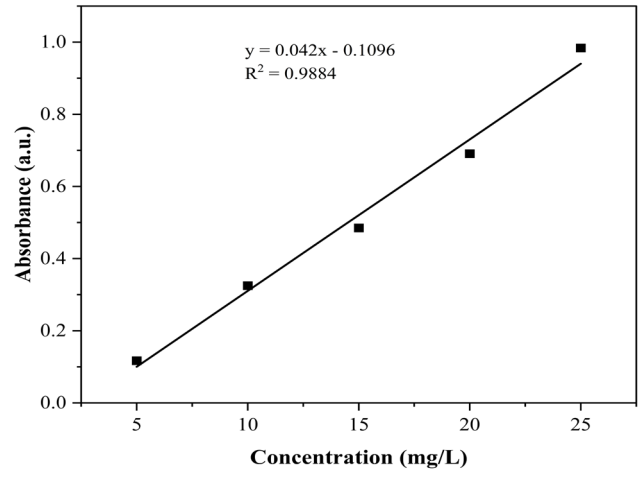

Figure 5. Calibration curve of methylene blue standard solution

Based on the regression equation of the methylene blue calibration curve, the surface area of durian peel activated carbon was 67.758 m^2/g at 0.3 M H_3PO_4, 70.040 m^2/g at 0.4 M, and 71.844 m^2/g at 0.5 M.

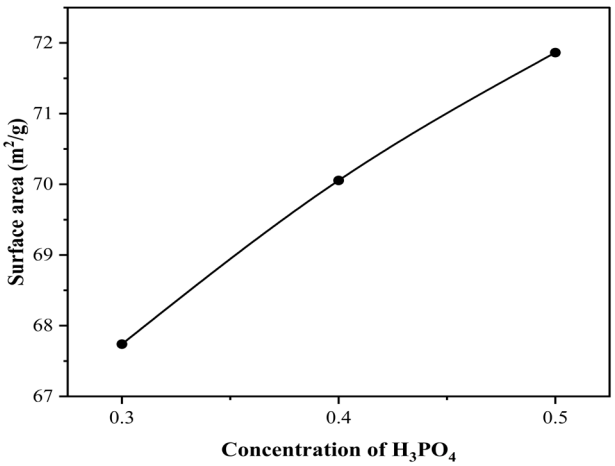

Figure 6. Surface area test results of durian peel activated carbon activated with phosphoric acid

Based on **Figure 6**, the calculated surface area values increased with increasing H_3PO_4 concentration. The highest value was obtained at an H_3PO_4 concentration of 0.5 M. Since the highest surface area value was obtained at 0.5 M H_3PO_4, this sample was selected for further characterization analyses.

The surface area values obtained in this study ranged from 67.758 to 71.844 m^2/g and were calculated using the methylene blue adsorption method. Since the calculation is based on the adsorption of methylene blue molecules onto the carbon surface, the resulting values represent an estimated surface area rather than a direct measurement of pore characteristics. Therefore, further analysis using other characterization methods may be useful to provide a more comprehensive description of the surface properties of the activated carbon.

Characterization

FTIR Characterization of activated carbon

Fourier Transform Infrared Spectroscopy (FTIR) characterization was carried out to identify the functional groups present on the surface of durian peel activated carbon activated with phosphoric acid (H_3PO_4). The FTIR spectrum exhibited several characteristic absorption bands, indicating the presence of specific functional groups on the activated carbon surface.

The broad absorption band at 3408 cm^{-1} is attributed to O–H stretching vibrations associated with hydroxyl groups, phenolic groups, or adsorbed water

on the activated carbon surface. The absorption band at 2924 cm^{-1} corresponds to aliphatic C–H stretching vibrations derived from residual organic components of the biomass. Absorption bands observed in the 1693–1610 cm^{-1} region is assigned to aromatic C=O and C=C functional groups, indicating the presence of aromatic carbon structures formed during the carbonization process.

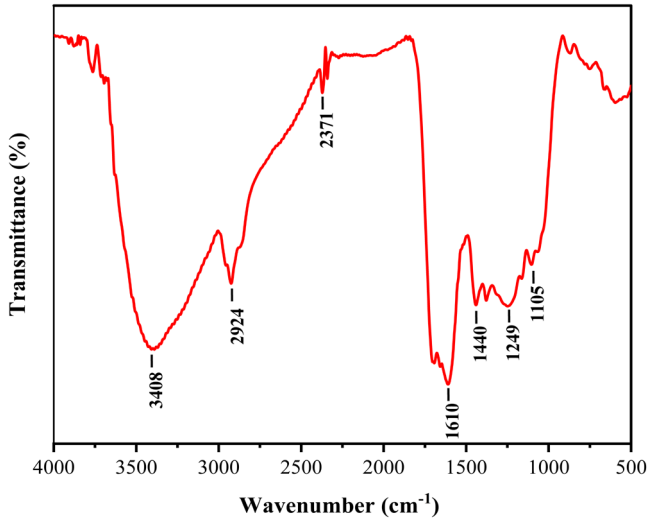

Figure 7. FTIR Spectrum of H_3PO_4-activated carbon

The presence of phosphate-related groups is indicated by absorption bands at 1249 cm^{-1} and in the 1163–1105 cm^{-1} region, which are associated with P=O and P–O–C vibrational modes. These bands are commonly observed in H_3PO_4-activated carbon and indicate the presence of phosphate-containing species on the carbon surface. In addition, the absorption band in the 657–596 cm^{-1} region is attributed to P–O bending vibrations associated with phosphate or polyphosphate compounds.

Previous studies have reported that H_3PO_4-activated carbon contains O–H, aromatic C=C, and phosphate-related functional groups in the 1300–900 cm^{-1} region [20]. Similar functional groups have also been observed in H_3PO_4-activated durian peel activated carbon [25]. The FTIR spectrum obtained in this study confirms the presence of oxygen-containing and phosphate-related functional groups on the surface of the activated carbon after the activation process

XRD characterization of activated carbon

X-ray diffraction (XRD) characterization was carried out to determine the structural characteristics of activated carbon after activation with phosphoric acid (H_3PO_4). This analysis was performed on the activated carbon prepared using 0.5 M H_3PO_4, which exhibited the best adsorption performance among the samples studied.

The XRD results in **Figure 8** show a broad diffraction peak at 2θ = 21.08°. This peak indicates that the activated carbon is predominantly amorphous with an irregular carbon structure. Such an amorphous nature is a typical characteristic of biomass-derived activated carbon and contributes to pore formation in carbon materials. H_3PO_4-activated carbon generally exhibits a broad diffraction pattern in the 2θ range of approximately 20–30°, confirming the dominance of the amorphous carbon phase [7].

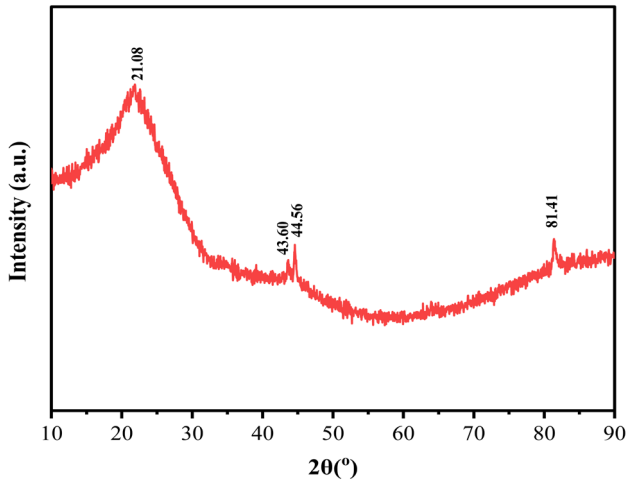

Figure 8. XRD Diffraction pattern of H_3PO_4-activated carbon

The activated carbon also exhibits weak diffraction peaks at 2θ = 43.60° and 44.56°. Diffraction features in this region have been reported for carbon materials and are commonly discussed with reference to graphite-related carbon structures based on JCPDS/PDF No. 41-1487 [26,27]. However, the relatively low intensity of these peaks suggests that the degree of structural ordering is limited and that these features are not dominant in the diffraction pattern.

Similar diffraction patterns, characterized by a broad peak in the range of 20–30° together with weak reflections near 43°, have been reported for activated carbon materials derived from biomass precursors [26, 27]. These results indicate that the activated carbon produced in this study is dominated by an amorphous carbon phase with only a limited degree of structural ordering.

Point of zero charge (pHpzc) determination of durian peel activated carbon

The pHpzc (point of zero charge) was determined to identify the pH at which the surface of activated carbon is electrically neutral. The pHpzc value describes changes in the surface charge of activated carbon as a function of solution pH and helps explain

the interaction between the adsorbent and adsorbate during adsorption. At pH values below the pHpzc, the activated carbon surface tends to be positively charged, whereas at pH values above the pHpzc, the surface becomes negatively charged [28].

Based on **Figure 9**, the intersection between the ΔpH curve and the initial pH occurred at pH 4.1. Therefore, the pHpzc value of durian peel activated carbon activated with H_3PO_4 was determined to be 4.1. This result indicates that the surface charge of the activated carbon changes around this pH. The relatively low pHpzc value may be related to the presence of oxygen-containing and phosphate functional groups introduced during H_3PO_4 activation.

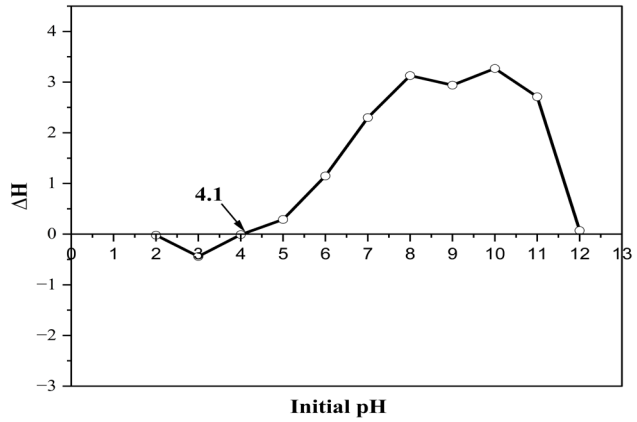

Figure 9. pHpzc curve of durian peel activated carbon activated with 0.5 M H_3PO_4

Activation with H_3PO_4 is known to alter the surface chemistry of activated carbon through the introduction of oxygen-containing and phosphate groups. The presence of these groups affects the surface charge of the carbon and influences its interaction with dissolved species in solution [25].

The pHpzc value obtained in this study suggests that the activated carbon surface is positively charged under acidic conditions. This characteristic is favorable for the adsorption of anionic dyes such as Direct Red 80 because electrostatic attraction can occur between the positively charged carbon surface and negatively charged dye molecules

Adsorption test of Direct Red 80

The concentration of Direct Red 80 was determined using a UV–Vis spectrophotometer based on a calibration curve of the standard solution at a maximum wavelength (λmax) of 528 nm. Based on **Figure 10**, the Direct Red 80 calibration curve shows a linear relationship between concentration and absorbance, with a regression equation of y = 0.0316x + 0.0057 and a coefficient of determination (R^2) of 0.9995. An R^2 value close to 1 indicates excellent linearity between concentration and absorbance, allowing the calibration curve to be used to determine the residual concentration of Direct Red 80 during the adsorption process.

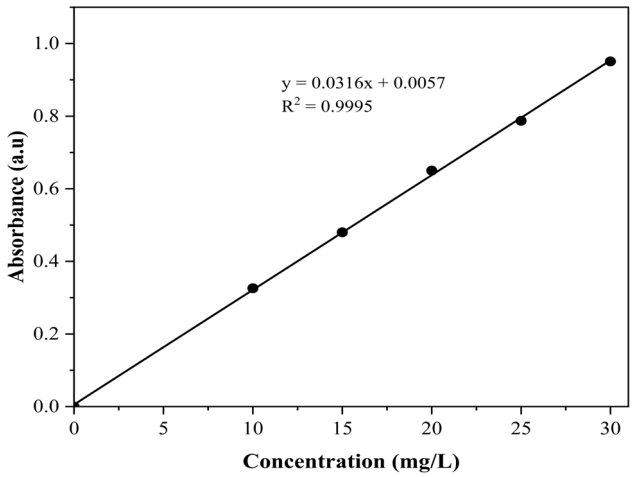

Figure 10. Direct Red 80 calibration curve

Based on **Figure 11**, the adsorption efficiency of Direct Red 80 onto H_3PO_4-activated durian peel carbon decreased with increasing solution pH. The highest adsorption efficiency was observed at pH 2 (66.72%), followed by 55.97% at pH 3 and 53.17% at pH 4. A more pronounced decrease was observed at pH 5 (38.45%), reaching the lowest value at pH 6 (28.33%). These results indicate that acidic conditions are more favorable for the adsorption of Direct Red 80 onto the activated carbon.

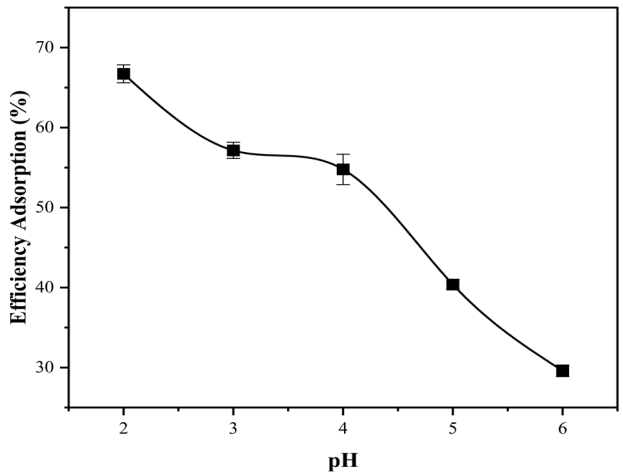

Figure 11. Effect of pH on the adsorption efficiency of Direct Red 80

Adsorption of anionic dyes is generally more favorable at low pH due to stronger electrostatic interactions between the adsorbent and adsorbate. The

higher adsorption under acidic conditions is associated with the surface charge of activated carbon, which is influenced by its pHpzc value of 4.1. At pH values below the pHpzc, the surface of activated carbon becomes positively charged, enhancing electrostatic attraction with anionic Direct Red 80 molecules. Direct Red 80 contains negatively charged sulfonate groups ($–SO_3^-$), which facilitate interaction with the positively charged adsorbent surface under acidic conditions. Increased protonation of the adsorbent surface further strengthens the attraction toward the anionic dye, thereby enhancing the adsorption capacity [29].

The decrease in adsorption efficiency at higher pH is attributed to the development of a negatively charged surface on the activated carbon due to the increased concentration of OH^- ions in solutions. This condition leads to electrostatic repulsion between the adsorbent surface and Direct Red 80 molecules, which are also negatively charged, resulting in reduced dye uptake. In addition, OH^- ions may compete with dye molecules for adsorption sites on the adsorbent, thereby decreasing the adsorption capacity under alkaline conditions. Similar behavior has been reported in previous studies on the adsorption of anionic dyes using activated carbon-based adsorbents[30, 31]. In addition, changes in solution pH during the adsorption process may also influence the adsorption behavior of Direct Red 80. Further studies involving pH monitoring before and after adsorption are recommended to better evaluate possible experimental effects.

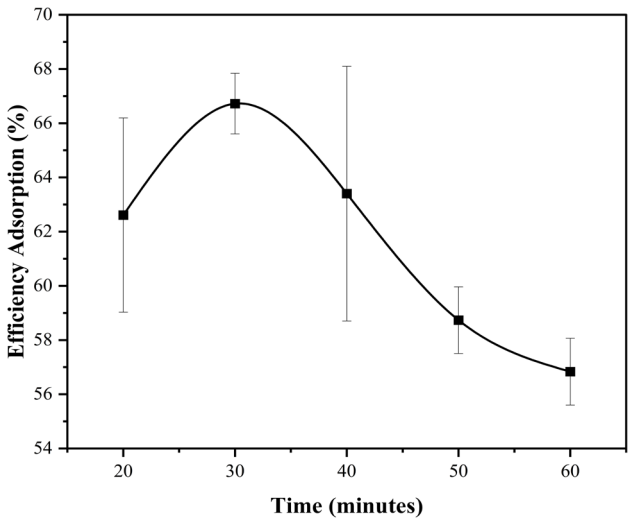

Figure 12. Effect of contact time on the adsorption efficiency of Direct Red 80

Based on **Figure 12**, the adsorption efficiency of Direct Red 80 onto H_3PO_4-activated durian peel carbon initially increased with contact time and then gradually decreased after reaching the maximum value. The adsorption efficiency was 62.61% at 20 min and increased to 66.72% at 30 min. It subsequently decreased to 63.40% at 40 min, 58.73% at 50 min, and 56.84% at 60 min. The results indicate that the highest adsorption efficiency under the investigated conditions was obtained at a contact time of 30 min.

The increase in adsorption efficiency during the initial stage can be attributed to the availability of abundant active sites on the surface of the activated carbon, allowing effective interaction between the adsorbent and Direct Red 80 molecules. As contact time increased, a greater number of dye molecules came into contact with the adsorbent surface, resulting in more effective adsorption until the maximum adsorption efficiency was achieved [32].

After 30 min, the adsorption efficiency showed a gradual decline. This behavior suggests that extending the contact time beyond the optimum value did not provide a significant improvement in adsorption performance under the experimental conditions employed. The error bars shown in **Figure 12** indicate some variability among replicate measurements, particularly at intermediate contact times. Since no desorption experiment was conducted in this study, the observed decrease cannot be conclusively attributed to a specific mechanism. Nevertheless, the results demonstrate that a contact time of 30 min was sufficient to achieve effective adsorption of Direct Red 80 onto the activated carbon.

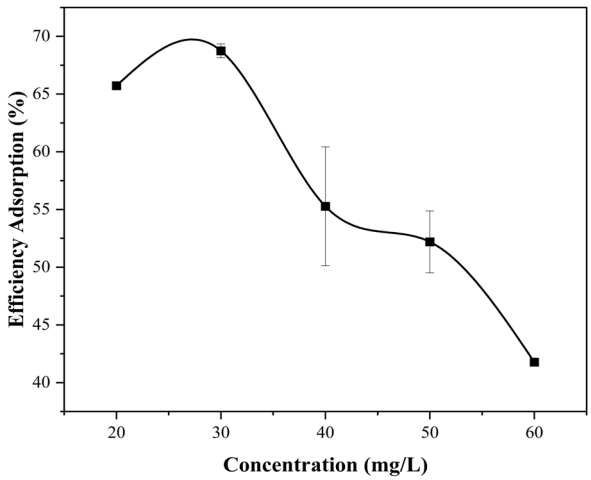

Figure 13. Effect of initial concentration on adsorption efficiency

Based on **Figure 13**, the adsorption efficiency of Direct Red 80 onto H_3PO_4-activated durian peel carbon varied with the initial dye concentration. The adsorption efficiency was 66.72% at 20 ppm and increased slightly to 68.41% at 30 ppm. It then

decreased to 51.63% at 40 ppm, increased again to 60.28% at 50 ppm, and finally decreased to 41.52% at 60 ppm. These results indicate that the initial dye concentration influenced the adsorption performance of the activated carbon toward Direct Red 80.

The highest adsorption efficiency was observed at 30 ppm, indicating that this concentration provided a favorable balance between the number of dye molecules present in solution and the available adsorption sites on the adsorbent surface. At lower concentrations, sufficient active sites were available to accommodate the dye molecules, resulting in relatively high adsorption efficiencies. As the concentration increased further, the number of dye molecules became greater relative to the available adsorption sites, which may have reduced the adsorption efficiency.

The fluctuations observed at intermediate concentrations are reflected by the error bars presented in **Figure 13**, indicating variability among replicate measurements. Such behavior may be associated with factors including partial saturation of adsorption sites, aggregation of dye molecules, or multilayer adsorption phenomena at certain concentrations. However, additional experimental evidence would be required to confirm the contribution of these effects. Similar observations have been reported in studies on dye adsorption using biomass-based adsorbents [32].

Adsorption kinetic

Adsorption kinetics were used to determine the most suitable adsorption model based on the relationship between contact time and the adsorption capacity of the adsorbent for the adsorbate. In this study, pseudo-first-order and pseudo-second-order kinetic models were applied to analyze the adsorption process of Direct Red 80 onto H_3PO_4-activated durian peel carbon. The adsorption kinetic parameters are presented in **Table 1**.

Table 1. Kinetic parameters of direct red 80 adsorption

Kinetic Model	Parameter	Value
Pseudo First Order	R^2	0.2292
	k_1 (min^{-1})	0.0066
	qe (mg/g)	0.4591
Pseudo Second Orde	R^2	0.9916
	k_2 (g/mg.min)	0.0397
	qe (mg/g)	5.3361

Based on the results of the adsorption kinetics analysis, the pseudo-second-order model exhibited a higher coefficient of determination (R^2) than the pseudo-first-order model. The R^2 value of 0.9916 indicates that the pseudo-second-order model is more suitable for describing the adsorption process of Direct Red 80 onto H_3PO_4-activated durian peel carbon. In contrast, the pseudo-first-order model showed a much lower R^2 value of 0.2292, indicating a poor fit to the experimental data. The adsorption capacity (qe) calculated using the pseudo-second-order model was 5.336 mg/g, which is relatively close to the experimental qe value (6.672 mg/g).

The suitability of the pseudo-second-order model indicates that the adsorption process proceeds effectively until equilibrium is reached on the adsorbent surface. These findings are consistent with previous studies reporting that the pseudo-second-order model provides a better fit than the pseudo-first-order model for dye adsorption using biomass-based activated carbon [29]. Other studies have also shown that the pseudo-second-order model generally yields higher coefficients of determination for dye adsorption using activated carbon compared to the pseudo-first-order model [33].

Adsorption isotherm

Adsorption isotherms are used to determine the characteristics of interactions between the adsorbent and adsorbate under equilibrium conditions. In this study, the Langmuir and Freundlich isotherm models were applied to analyze the adsorption process of Direct Red 80 onto H_3PO_4-activated durian peel carbon. The adsorption isotherm parameters are presented in **Table 2**.

Table 2. Adsorption isotherm parameters of direct Red 80

Isotherm Model	Parameter	Direct Red 80
Langmuir	R^2	0.9713
	Qm (mg/g)	15.31
	K_L (L/mg)	0.157
Freundlich	R^2	0.7728
	K_f	4.02
	N	2.88

Based on the results of the adsorption isotherm analysis, the Langmuir model exhibited a higher coefficient of determination (R^2) than the Freundlich model. The Langmuir model showed an R^2 value of 0.9713, indicating that it is more appropriate for describing the adsorption process of Direct Red 80 onto H_3PO_4-activated durian peel carbon. In contrast, the Freundlich model showed a lower R^2 value of 0.7728, indicating a poorer fit to the experimental data. The suitability of the Langmuir model indicates that the adsorption process occurs as monolayer coverage on a relatively homogeneous adsorbent surface. The maximum adsorption capacity (Q_m) of 15.31 mg/g

reflects the ability of H_3PO_4-activated durian peel carbon to adsorb Direct Red 80 dye. These findings are consistent with previous studies reporting that the Langmuir model provides a better fit than the Freundlich model for dye adsorption using biomass-based activated carbon [34]. The Langmuir model has also been shown to describe dye adsorption on homogeneous surfaces through the formation of a single adsorbate layer [35].

CONCLUSION

Durian peel carbon activated with H_3PO_4 was prepared through microwave carbonization followed by acid treatment using phosphoric acid. The resulting material met the requirements of SNI 06-3730-1995, exhibited a predominantly amorphous structure, and contained O–H, aromatic C=C, and phosphate functional groups. Activation with 0.5 M H_3PO_4 produced the best adsorbent, with an iodine adsorption capacity of 1192.86 mg/g and a surface area of 71.84 m^2/g determined by the methylene blue adsorption method.

The adsorbent showed good performance for Direct Red 80 removal, with the highest adsorption efficiencies observed at pH 2, a contact time of 30 min, and an initial dye concentration of 30 ppm. The pHpzc value was 4.1, indicating that adsorption was favored under acidic conditions. Kinetic analysis showed that the adsorption process followed the pseudo-second-order model, while the Langmuir isotherm provided the best fit to the equilibrium data with a maximum adsorption capacity of 15.31 mg/g.

These findings indicate the potential of durian peel-derived carbon as a low-cost adsorbent for dye removal from aqueous solutions. However, the surface area was determined using the methylene blue adsorption method, and BET analysis was not performed. Further studies are recommended to optimize the activation process and evaluate the adsorption performance using real textile wastewater

REFERENCES

[1] S. Hsiao, S. You, C. Wang, J. Deng, and H. Hsi, "Adsorption of Volatile Organic Compounds and Microwave Regeneration on Self-prepared High-surface-area Beaded Activated Carbon," *Aerosol and Air Quality Research*, vol. 22, no. 6, pp. 1–15, 2020, doi:doi.org/10.4209/aaqr.220010.

[2] M. Kadhom, N. Albayati, H. Alalwan, and M. Al-Furaiji, "Removal of dyes by agricultural waste," *Sustainable Chemistry and Pharmacy*, vol. 16, no. January, p. 100259, 2020, doi: 10.1016/j.scp.2020.100259.

[3] I. Apriani, D. H. Y. Yanto, P. L. Hariani, H. Widjajanti, and O. D. Nurhayat, "Potential of White Rot Fungi from Berbak-Sembilang National Park, Indonesia for Decolorization and Detoxification Commercial Direct Dyes," *Trends in Sciences*, vol. 21, no. 6, pp. 1–12, 2024, doi: 10.48048/tis.2024.7610.

[4] S. Kanchi, K. Bisetty, G. Kumar, and M. I. Sabela, "Robust adsorption of Direct Navy Blue-106 from textile industrial effluents by bio-hydrogen fermented waste derived activated carbon: Equilibrium and kinetic studies," *Arabian Journal of Chemistry*, vol. 10, pp. S3084–S3096, 2017, doi: 10.1016/j.arabjc.2013.11.050.

[5] R. Tambun, B. Haryanto, V. Alexander, D. R. Manurung, and A. P. Ritonga, "Durian peel (Durio zibethinus) utilization as an adsorbent in the purification of acidified crude glycerol," *South African Journal of Chemical Engineering*, vol. 49, no. January, pp. 162–169, 2024, doi: 10.1016/j.sajce.2024.05.002.

[6] S. M. Yakout and G. Sharaf El-Deen, "Characterization of activated carbon prepared by phosphoric acid activation of olive stones," *Arabian Journal of Chemistry*, vol. 9, pp. S1155–S1162, 2016, doi: 10.1016/j.arabjc.2011.12.002.

[7] O. Oginni, K. Singh, G. Oporto, B. Dawson-Andoh, L. McDonald, and E. Sabolsky, "Effect of one-step and two-step H_3PO_4 activation on activated carbon characteristics," *Bioresource Technology Reports*, vol. 8, no. July, p. 100307, 2019, doi: 10.1016/j.biteb.2019.100307.

[8] Q. Han, J. Wang, B. A. Goodman, J. Xie, and Z. Liu, "High adsorption of methylene blue by activated carbon prepared from phosphoric acid treated eucalyptus residue," *Powder Technology*, vol. 366, pp. 239–248, 2020, doi: 10.1016/j.powtec.2020.02.013.

[9] I. Neme, G. Gonfa, and C. Masi, "Activated carbon from biomass precursors using phosphoric acid: A review," *Heliyon*, vol. 8, no. 12, p. e11940, 2022, doi: 10.1016/j.heliyon.2022.e11940.

[10] T. C. Chandra, M. M. Mirna, J. Sunarso, Y. Sudaryanto, and S. Ismadji, "Activated carbon from durian shell: Preparation and characterization," *Journal of the Taiwan Institute of Chemical Engineers*, vol. 40, no. 4,

pp. 457–462, 2009, doi: 10.1016/j.jtice.2008.10.002.

[11] S. Huda, R. Dwi, and L. Kurniasari, "Karakterisasi Karbon Aktif Dari Bambu Ori (Bambusa arundinacea) Yang Di Aktivasi Menggunakan Asam Klorida," *Jurnal Inovasi Teknik Kimia*, vol. 5, no. 1, pp. 22–27, 2020, doi: 10.31942/inteka.v5i1.3397.

[12] Y. A. B. Neolaka, E. B. S. Kalla, G. A. Malelak, and N. K. Rukman, "Adsorption Of Methylene Blue Using Acid Activated Green Color Natural Zeolite From Ende-Flores , Indonesia," *Rasayan Journal of Chemistry*, vol. 11, no. 2, pp. 494–504, 2018, doi: 10.31788/RJC.2018.1121994

[13] H. Lee, S. Fiore, and F. Berruti, "Biomass and Bioenergy Adsorption of methyl orange and methylene blue on activated biocarbon derived from birchwood pellets," *Biomass and Bioenergy*, vol. 191, no. September, p. 107446, 2024, doi: 10.1016/j.biombioe.2024.107446.

[14] E. Misran, M. Dani, D. Agustina, V. Pramananda, A. Faulina, and D. Valianty, "Results in Engineering Ultrasonic assisted adsorption of methylene blue using blood clam shell as a low-cost adsorbent," *Results in Engineering*, vol. 23, no. December 2023, p. 102715, 2024, doi: 10.1016/j.rineng.2024.102715.

[15] L. Ke, N. Zhou, Q. Wu, Y. Zeng, X. Tian, J. Zhang, L. Fan, R. Ruan, Y. Wang, "Microwave catalytic pyrolysis of biomass : a review focusing on absorbents and catalysts," *npj Materials Sustainability*, vol. 2, p. 24, 2024, doi: 10.1038/s44296-024-00027-7.

[16] A. Damayanti, R. Wulansarie, Z. A. S. Bahlawan, Suharta, M. Royana, M. W. N. N. Basuki, B. Nugroho, A. L. Andri, "Effects of Phosphate and Thermal Treatments on the Characteristics of Activated Carbon Manufactured from Durian (Durio zibethinus) Peel," *ChemEngineering*, vol. 7, no. 5, 2023, doi: 10.3390/chemengineering7050075.

[17] P. J. Wibawa, H. A. S. Ningrum, P. Damayanti, Z. U. F. Al-Hasan, Suhartana, and Pardoyo, "Sequentially citric acid-KMnO4-modified surface of activated carbon microparticles to enhance the capability of loading silver nanoparticles as a bacterial sensor material," *Diamond and Related Materials*, vol. 136, no. December 2022, 2023, doi: 10.1016/j.diamond.2023.109900.

[18] T. U. Vandana, B. K. Tripathy, R. K. Mishra, A. Sharma, and K. Mohanty, "A review on waste biomass-derived biochar: Production, characterisation, and advanced analytical techniques for pollutants assessment in water and wastewater," *Process Safety and Environmental Protection*, vol. 201, no. PA, p. 107505, 2025, doi: 10.1016/j.psep.2025.107505.

[19] S. Allende, Y. Liu, M. Adeel, and Z. Mohan, "Nitrite sensor using activated biochar synthesised by microwave - assisted pyrolysis," *Waste Disposal & Sustainable Energy*, vol. 5, no. 1, pp. 1–11, 2023, doi: 10.1007/s42768-022-00120-4.

[20] N. V Sych, S. I. Trofymenko, O. I. Poddubnaya, M. M. Tsyba, V. I. Sapsay, D. O. Klymchuk, A. M. Puziy, "Applied Surface Science Porous structure and surface chemistry of phosphoric acid activated carbon from corncob," *Applied Surface Science*, vol. 261, pp. 75–82, 2012, doi: 10.1016/j.apsusc.2012.07.084.

[21] J. Chagu and A. J. Mwakalesi, "Effects of phosphoric acid concentration on properties of activated carbon from Strychnos spinose fruit shells," *Scientific Reports*, vol. 16, p. 4009, 2026, doi: 10.1038/s41598-025-34098-w.

[22] H. Marsh and F. Rodriguez-reinoso, *Activated Carbon*, 1st ed. Amsterdam: Elsevier, 2006.

[23] P. Sriprom, W. Krusong, and P. Assawasaengrat, "Preparation of activated carbon from durian rind with difference activations and its optimization," *Journal of Renewable Materials*, vol. 9, no. 2, pp. 311–324, 2021, doi: 10.32604/jrm.2021.012560.

[24] R. K. Mishra, B. Singh, and B. Acharya, "A comprehensive review on activated carbon from pyrolysis of lignocellulosic biomass : An application for energy and the environment," *Carbon Resources Conversion*, vol. 7, no. 4, p. 100228, 2024, doi: 10.1016/j.crcon.2024.100228.

[25] Yuliusman, M. P. Ayu, A. Hanafi, and A. R. Nafisah, "Activated carbon preparation from durian peel wastes using chemical and physical activation," *AIP Conference Proceedings*, vol. 2230, no. May, 2020, doi: 10.1063/5.0002348.

[26] H. Peng, G. Hao, Z. Chu, Y. Lin, X. Lin, and Y. Cai, "RSC Advances a metal – organic framework as a lithium-ion battery," *RSC Advance*, vol. 7, pp. 34104–34109, 2017, doi: 10.1039/C7RA05090A.

[27] J. Serafin, B. Dziejarski, X. Vendrell, K. Kielbasa, and B. Michalkiewicz, "Biomass and Bioenergy Biomass waste fern leaves as a

material for a sustainable method of activated carbon production for CO 2 capture," *Biomass and bioenergy*, vol. 175, pp. 1-10, 2023, doi: 10.1016/j.biombioe.2023.106880.

[28] K. Y. Foo and B. H. Hameed, "Microwave-assisted preparation of oil palm fiber activated carbon for methylene blue adsorption," *Chemical Engineering Journal*, vol. 166, p. 5996422, 2011, doi: 10.1016/j.cej.2010.11.019.

[29] N. U. M. Nizam, M. M. Hanafiah, E. Mahmoudi, and A. A. Halim, "The removal of anionic and cationic dyes from an aqueous solution using biomass - based activated carbon," *Scientific Reports*, pp. 1–17, 2021, doi: 10.1038/s41598-021-88084-z.

[30] W. Boumya, M. Khnifira, A. Machrouhi, and M. Abdennouri, "Box – Behnken design for understand ing of adsorption behaviors of cationic and anionic dyes by activated carbon," *Desalination and Water Treatment*, vol. 212, pp. 204–211, 2021, doi: 10.5004/dwt.2021.26610.

[31] K. Azam, N. Shezad, I. Shafiq, P. Akhter, F. Akhtar, F. Jamil, S. Shafique, Y. Park, M. Hussain, "Chemosphere A review on activated carbon modifications for the treatment of wastewater containing anionic dyes," *Chemosphere*, vol. 306, no. July, p. 135566, 2022, doi: 10.1016/j.chemosphere.2022.135566.

[32] H. O. Chukwuemeka, O. Francis, K. E. Kovo, J. C. Nnaji, and A. G. Okereafor, "Adsorption of tartrazine and sunset yellow anionic dyes onto activated carbon derived from cassava sievate biomass," *Applied Water Science*, vol. 11, no. 2, pp. 1–8, 2021, doi: 10.1007/s13201-021-01357-w.

[33] Z. Harrache and M. Abbas, "Elimination of a cationic dye in aqueous solution by adsorption on activated carbon : Optimization of analytical parameters , modeling and thermodynamic study," *Journal of Engineered Fibers and Fabrics*, vol. 2, pp. 1–11, 2022, doi: 10.1177/15589250221134343.

[34] A. El Jery, H. S. K. Alawamleh, M. H. Sami, H. A. Abbas, S. S. Sammen, A. Ahsan, M. A. Imteaz, A. Shanableh, M. Shafiquzzaman, H. Osman, N. Al-Ansari, "Isotherms, kinetics and thermodynamic mechanism of methylene blue dye adsorption on synthesized activated carbon," *Scientific Reports*, pp. 1–12, 2024, doi: 10.1038/s41598-023-50937-0.

[35] J. Saleem, Z. Khalid, B. Moghal, S. Pradhan, and G. Mckay, "RSC Advances High-performance activated carbon from coconut shells for dye removal : study of isotherm and," *RSC Advance.*, vol. 14, pp. 33797–33808, 2024, doi: 10.1039/D4RA06287F.